Bridge modal identification based on successive variational mode decomposition using a moving test vehicle

Jiantao Li[1], Xinqun Zhu[2], and Jian Guo[1,3*]

[1]School of Civil Engineering, Zhejiang University of Technology, Hangzhou 310023, China

[2]School of Civil and Environmental Engineering, University of Technology Sydney, Broadway, NSW 2007, Australia

[3]Department of Bridge Engineering, Southwest Jiaotong University, Chengdu, China

[*]Corresponding author: Guoj@Vip.163.com

Abstract

Bridge modal identification using an instrumented vehicle as a moving sensor is promising but challenging. A key factor is to extract bridge dynamic components from vehicle responses measured when the bridge is operating. A new method based on an advanced adaptive signal decomposition technique, the successive variational mode decomposition (SVMD), has been developed to estimate the bridge modal parameters from the dynamic responses of a passing instrumented vehicle. When bridge-related dynamic components are extracted from the decomposition, the natural excitation technique (NExT) and/or random-decrement technique (RDT) based fitting methods are used to estimate the modal frequencies and damping ratios of the bridge. Effects of measurement noise, moving speed and vehicle properties on the decomposition are investigated numerically. The superiority of SVMD in the decomposition is verified by comparing to another adaptive decomposition technique, the singular spectrum decomposition (SSD). The results of the proposed method confirm that the bridge modal frequencies can be identified from bridge related components with high accuracy, while damping ratio is more sensitive to the random operational load. Finally, the feasibility of the proposed method for drive-by bridge monitoring is further verified by an in-situ experimental test on a cable-stayed bridge. The components relate to the bridge dynamic responses are successfully extracted from vehicle responses.

Keywords: Operational modal identification, adaptive signal decomposition, SVMD, SSD

1. Introduction

Bridge modal identification using instrumented sensing vehicle has drawn great attention due to its significant potential for quick scan of bridge structural health conditions (Yang et al., 2020; Locke et al., 2020). The sensing vehicle measuring bridge dynamic responses under operational conditions is more convenient and cost-effective compared to the conventional fixed sensing networks mounted on the structure. Modal parameters identified from vehicle responses can be used to assess the health conditions of bridge (Mei et al., 2019). However, the extraction of useful dynamic information from vehicle responses for bridge health monitoring is not trivial (Hester and González, 2017; Tan et al., 2019). The vertical dynamic response of vehicle passing over a bridge is a multi-component signal mainly including the bridge dynamic component, vehicle dynamic component and driving component (Yang et al., 2004). When bridge surface

roughness is considered, the vehicle related dynamic component is amplified and the bridge related dynamic information becomes less visible.

To enhance the drive-by bridge modal identification, signal processing techniques have been used to reduce the effects of road surface roughness and to extract bridge related dynamic information. Wavelet transform based methods have been used to separate the bridge dynamic information from the vehicle dynamic response (Jian et al., 2020; Li et al., 2021). However, the selection for the optimal wavelet parameters is an arbitrary process that may cause uncertainties (Tan et al., 2020). Empirical mode decomposition (EMD) as a data-adaptive technique has been used to decompose vehicle response (Yang and Chang, 2009; Yang and Lee, 2018) into a set of intrinsic mode functions (IMFs). The recovered IMFs by repeated siftings process in EMD made bridge frequencies more visible in the first few IMFs. The IMFs extracted from vehicle response were used as damage indicators of bridge structure (O'Brien et al., 2017; Kildashti et al., 2020). EEMD method introduced by Wu and Huang (2009) to address the mode mixing problem of the EMD was used to identify bridge modal frequencies from vehicle response (Zhu and Malekjafarian, 2019). The results showed that EEMD method provided better performance on the decomposition of vehicle responses compared to EMD. Singular spectrum analysis (SSA) (Elsner and Tsonis, 1996) is another powerful technique for time series decomposition and eigenvalue identification that has been applied in the field of drive-by bridge modal identification. Yang et al. (2013) applied SSA method to identify the bridge frequencies from the test vehicle response. A combination of SSA with band-pass filter can filter out the vehicle-related dynamic components to improve the scan of bridge modal parameters. Li et al. (2019a) proposed a drive-by blind modal identification method (SSA-BSS) by combining SSA and second-order blind identification. However, SSA method requires manual selection of the embedding length. A new adaptive method, singular spectrum decomposition (SSD), for decomposing time series into narrow-banded components was proposed in (Bonizzi et al., 2014). The method is originated from SSA with an automated choice of fundamental parameters. SSD method has been shown to retrieve different components concealed in the data accurately to many fields. However, to the best knowledge of the authors, SSD has not been used to analyze vehicle responses for drive-by bridge inspection.

Moreover, Dragomiretskiy and Zosso (2014) proposed the variational mode decomposition (VMD), a noniterative and adaptive signal processing method. Due to its solid mathematical theoretical foundation compared with EMD, VMD-based methods have been used in different areas, such as the analysis of seismic signal (Li et al., 2018), underwater acoustic signal (Li et al., 2019b), structural system identification (Ni et al., 2018) and load data of mechanical systems (Fu et al., 2020). Tian and Zhang (2020) utilized VMD to decompose vehicle-induced bridge responses into IMFs to extract dynamic properties of the VBI coupled system. Yang et al. (2021) used VMD to extract the mono-components from contact-point responses of a VBI model to identify the frequencies and damping ratios of the bridge. The results demonstrated that VMD performed more efficiently and elegantly than EMD/EEMD in extracting the mono-component responses. Despite of its extensive application, the performance of

VMD is greatly affected by the manually preset mode number and mode frequency bandwidth control parameter (Zhang et al., 2018). Therefore, a novel successive variational mode decomposition (SVMD) method (Nazari and Sakhaei, 2020) is adopted which extracts the components successively and does not need to know the number of modes.

From the above discussion, it can be seen that SVMD has great potential to decompose vehicle responses into meaningful mono-components for bridge modal identification using instrumented vehicle. Therefore, this study investigates its performance in the decomposition of vehicle responses for operational drive-by identification of bridge. The bridge related components are extracted to identify frequencies and damping ratios by incorporating NExT (James et al., 1993) and/or RDT (Ibrahim, 1977) based modal identification algorithms, respectively. Moreover, the extracted components are further explored to estimate the contact-point response of the bridge at the contact point of vehicle and bridge.

The rest of the paper is organized as follows. Section 2 presents the vehicle bridge interaction model that describes the dynamics of bridge structure under operational moving load and the response measurement of sensing vehicle. Section 3 briefly introduces the SVMD for the decomposition of vehicle responses. The NExT and RDT to be used for damping ratio identification are also described. Extensive numerical study is conducted in Section 4 to demonstrate the decomposition results of the adaptive techniques. Feasibility of the incorporated damping ratio identification methods is investigated. Finally, the vehicle response measured from an in-situ vehicle-bridge interaction test is used to further verify the effectiveness of the decomposition methods which is followed by conclusions.

2. Vehicle-bridge interaction model considering operational load

For the implementation of vibration-based bridge health monitoring, sufficient external load is usually required to excite the bridge structure to a certain extent (Makki Alamdari et al., 2021). For a bridge subjected to a medium to large volume of random operational traffic, the spatio-temporal load pattern can be modeled as a random white noise with sufficient accuracy (Sadeghi Eshkevari et al., 2020). Therefore, the VBI model considered for bridge modal identification is shown in Figure 1. The moving load P in the figure represents the operational load and a widely used single-degree-of-freedom quarter car is utilized as the instrumented sensing vehicle. The acceleration response measured from the sensing vehicle is used for bridge modal identification. The operational load enters the bridge ahead of the sensing vehicle with a moving speed v_1 and the speed of the sensing vehicle is v_2.

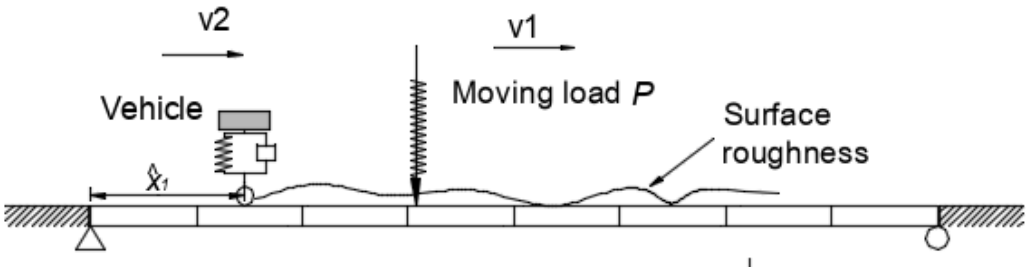

Figure 1 The model of drive-by bridge inspection in operational condition

2.1 Bridge model under operational load

The simply supported bridge with a length L can be modelled with finite element model. When the moving operational load $P(t)$ is incorporated into the bridge system, the motion of equation of bridge can be written as

$$\mathbf{M}_b\ddot{\mathbf{d}}_b(t) + \mathbf{C}_b\dot{\mathbf{d}}_b(t) + \mathbf{K}_b\mathbf{d}_b(t) = \mathbf{H}_r(t)P(t) \quad (1)$$

where $\mathbf{M}_b$, $\mathbf{C}_b$, and $\mathbf{K}_b$ are the mass, damping, and stiffness matrices of the bridge, respectively; $\ddot{\mathbf{d}}_b$, $\dot{\mathbf{d}}_b$, and $\mathbf{d}_b$ are the acceleration, velocity, and displacement responses at the element nodes of the bridge, respectively; $\mathbf{H}_r(t)P(t)$ is the equivalent nodal load vector for the finite element analysis. $\mathbf{H}_r(t)$ is based on the Hermitian cubic interpolation function for the calculation of equivalent nodal force from moving load $P(t)$. The entries of $\mathbf{H}_r(t)$ are zeros except at the degrees-of-freedom (DOFs) corresponding to the nodal displacements of the beam element on which the load is acting, with

$$\mathbf{H}_r = \{0 \dots 0 \dots \boldsymbol{H}_1 \dots 0\}^T \in R^{NN\times 1} \quad (2)$$

where *NN* is the total number of DOFs for the bridge model; the shape function $\boldsymbol{H}_1$ evaluates the moving load on the *j-th* beam element and its components are given as

$$\boldsymbol{H}_1 = \begin{Bmatrix} 1 - 3\left(\frac{\bar{x}_1(t) - (j-1)l_e}{l_e}\right)^2 + 2\left(\frac{\bar{x}_1(t) - (j-1)l_e}{l_e}\right)^3 \\ (\bar{x}_1(t) - (j-1)l_e)\left(\frac{\bar{x}_1(t) - (j-1)l_e}{l_e} - 1\right)^2 \\ 3\left(\frac{\bar{x}_1(t) - (j-1)l_e}{l_e}\right)^2 - 2\left(\frac{\bar{x}_1(t) - (j-1)l_e}{l_e}\right)^3 \\ (\bar{x}_1(t) - (j-1)l_e)\left(\left(\frac{\bar{x}_1(t) - (j-1)l_e}{l_e}\right)^2 - \left(\frac{\bar{x}_1(t) - (j-1)l_e}{l_e}\right)\right) \end{Bmatrix}^T$$

with $(j-1)l_e \le \bar{x}_1(t) \le jl_e$ and l_e is the length of finite element for the moving load on the *j-th* finite element.

2.2 Dynamics of the sensing vehicle

The vehicle is used as a moving sensor to measure the dynamic response of bridge under operational load $P(t)$. The vehicle parameters are: m_v the mass of vehicle, k_s and c_s the stiffness and damping of suspension spring and damper, respectively. The vehicle mass is very small compared to that of the bridge in this study. Its dynamic

effects on the bridge are neglected (Kong et al., 2014). The equation of motion of vehicle can be expressed as

$$m_v\ddot{y}_v(t) + c_v\dot{y}_v(t) + k_v y_v(t) = F_{cp}(t) \tag{3}$$

where y_v is the displacement response of vehicle; $F_{cp}(t) = k_v d_{cp}(t) + c_v\dot{d}_{cp}(t)$; $d_{cp}(t) = w(\hat{x}_1(t), t) + r(\hat{x}_1(t))$ is the displacement input to the sensing vehicle at location $\hat{x}_1(t)$ and $\dot{d}_{cp}(t)$ is its time derivative. The operational load moves over the bridge with a speed v_1 and it enters the bridge with a distance L_{ap} ahead of the sensing vehicle. The speed of operational load can be selected arbitrarily to simulate random excitation to bridge. Based on Eq.(1), the operational load is transformed to the equivalent nodal force at the nodes of the bridge beam elements. It can be viewed as applying the random load uniformly along the bridge span to consider its spatio-temporal characteristics (Sadeghi Eshkevari et al., 2020). Therefore, the moving speed of the operational load is simply set as $v_1 = L/(L + L_{ap})\, v_2$. Newmark-beta method is used to solve the Eqs. (1) and (3) to obtain the dynamic responses of the bridge structure and sensing vehicle.

2.3 Model of road surface roughness pattern

A widely used random roughness surface simulated based on ISO-8606 (1995) is considered. The random roughness in time domain can be given as follows (Henchi et al., 1998):

$$r(x) = \sum_{i=1}^{N_f} \sqrt{4S_d(f_i)\Delta f}\cos(2\pi f_i x + \theta_i) \tag{4}$$

where $S_d(f)$ is the displacement power spectral density of road surface roughness; $f_i = i\Delta f$ is the spatial frequency(cycles/m); $\Delta f = \frac{1}{N_f \Delta}$, and Δ is the distance interval between successive ordinates of the surface profile; N_f is the number of data points; θ_i is a set of independent random phase angle uniformly distributed between 0 and 2π. The degree of road roughness is determined by the $S_d(f_0)$ value, where $f_0 (= 0.1\ \text{cycles/m})$ is the reference spatial frequency. Class A road roughness defined using specified $S_d(f_0)$ value in ISO specification is considered. The roughness pattern in time and frequency domains are given in Figure 2.

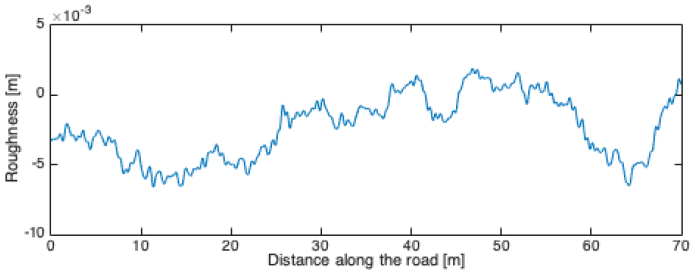

(a) Road roughness in time domain

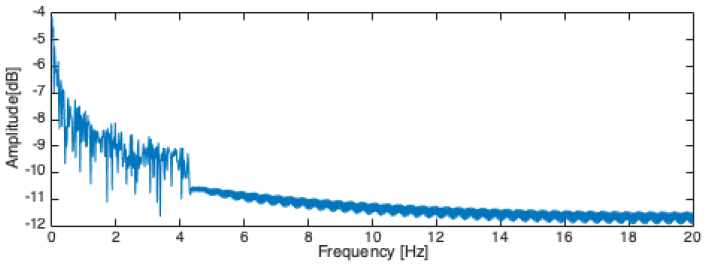

(b) PSD of the roughness

Figure 2. Road roughness profiles and the power spectrum density (PSD)

3. Bridge modal identification based on adaptive signal decomposition form a test vehicle

3.1 Successive variational mode decomposition

For the multi-component vehicle response with N data points, $\ddot{y}_v(t)$, its mono-components can be separated using SVMD iteratively. Unlike the VMD that finds IMFs simultaneously, the SVMD is performed to decompose signal into IMFs one after the other by successively applying variational mode extraction (Nazari and Sakhaei, 2018). This procedure is continued until all modes are extracted. Assume that the signal $\ddot{y}_v(t)$ is decomposed into two parts: the k-th mode $u_k(t)$ and the residual signal $y_r(t)$ as follows:

$$\ddot{y}_v(t) = u_k(t) + y_r(t) \tag{5}$$

where $y_r(t)$ contains the sum of previously obtained modes and the un-processed part of signal $y_u(t)$ as

$$y_r(t) = \sum_{i=1}^{k-1} u_i(t) + y_u(t) \tag{6}$$

The decomposition method is based on the following four criteria

(1) Each mode should be compact around its center frequency. The k-th mode minimizes the following criterion:

$$J_1 = \left\| \partial_t \left[\left(\delta(t) + \frac{j}{\pi t} \right) * u_k(t) \right] e^{-j\omega_k t} \right\|_2^2 \tag{7}$$

where $j = \sqrt{-1}$, ∂_t denotes the derivative with respect to time, $*$ the convolution operation, $\|\blacksquare\|$ the L^2-norm and ω_L is the center frequency of the k-th mode.

(2) The energy of the residual signal $y_r(t)$ should be minimized at frequencies where $u_k(t)$ has effective components. This constraint is realized by using a proper filter $\hat{\beta}_k(\omega)$ with frequency response of :

$$\hat{\beta}_k(\omega) = \frac{1}{\alpha(\omega - \omega_k)^2} \tag{8}$$

To get minimized spectral overlap between $y_r(t)$ and $u_k(t)$, the energy of filtered $y_r(t)$ by $\hat{\beta}_k(\omega)$ should be minimized. The following criterion needs to be realized:

$$J_2 = \|\beta_k(t) * y_r(t)\|_2^2 \tag{9}$$

where $\beta_k(t)$ is the impulse response of the filter $\hat{\beta}_k(\omega)$.

(3) Besides the minimization of criteria J_1 and J_2, $u_k(t)$ should have less energy at frequencies around the center frequencies of the previously obtained modes. This constraint can be satisfied using proper filters with the frequency responses as:

$$\hat{\beta}_i(\omega) = \frac{1}{\alpha(\omega-\omega_i)^2}; i = 1,2,\dots,k-1 \quad (10)$$

This added criterion is represented as follows:

$$J_3 = \sum_{i=1}^{k-1} \|\beta_i(t) * y_r(t)\|_2^2 \quad (11)$$

where $\beta_i(t)$ is the impulse response of the filter $\hat{\beta}_i(\omega)$.

(4) The last constrain is to guarantee complete reconstruction of $\ddot{y}_v(t)$ from k modes and the un-processed part of the signal:

$$\ddot{y}_v(t) = u_k(t) + y_u(t) + \sum_{i=1}^{k-1} u_i(t) \quad (12)$$

When k-1 modes are known, the problem of extracting the k-th mode can be expressed as a constrained minimization problem, in which a combination of J_1, J_2 and J_3 is minimized subject to the constrain of

$$\min_{u_L.\,\omega_L.\,y_r} \{\alpha J_1 + J_2 + J_3\} \quad \text{subject to: } u_k(t) + y_r(t) = \ddot{y}_v(t) \quad (13)$$

where α is a parameter for balancing J_1, J_2 and J_3, which can be solved through Lagrangian multiplier method. The weighting parameter α is one of the most important parameters of SVMD. A simple heuristic method to change α in each iteration is used to avoid the problems related to low or high value of α. The algorithm of SVMD with varying α is presented in (Nazari and Sakhaei, 2020).

3.2 Bridge modal identification using a moving test vehicle

In this study, it is assumed that the properties of sensing vehicle are known, and vehicle's frequencies are not coincided with those of bridge. Therefore, the bridge related dynamic mono-components can be extracted from vehicle response for the identification of bridge modal frequency and damping ratio (Yang et al. 2021). When the mono-components related to the bridge dynamic modes are extracted, the frequency can be easily identified and the damping ratio for each mode can be estimated by the least-squares fitting an exponential decay to the envelop of the impulse response function (IRF) of the system. Since the IRF is not directly available, the NExT and/or RDT are applied to extract the impulse response function from the mono-component.

The underlying theory for the NExT is that the auto- and cross-correlation function of output data for a system subjected to white-noise input are similar to the impulse response. The correlation function can be estimated using direct procedure with time domain data or via calculating spectral density functions. The calculation of correlation function requires a preset time lag *T*. While the principle of RDT is to estimate random decrement signatures by averaging time segments of the responses. These segments are selected under certain triggering conditions. For the application of RDT, two key parameters, i.e., the trigger threshold Φ and time lag *T* to determine the segment number, need to be preset. The most used triggering conditions are level-crossing, positive point, local extrema, and zero-up crossing. In this study, the level-crossing triggering condition is utilized with the recommendation of $\Phi = \sqrt{2}\sigma$, where σ is the standard deviation of the signal. The outcome of the fitting procedure depends on the number of cycles considered within the IRF. It is better to have a sufficient length of the time lag *T* to cover the low frequencies of the structure (Kordestani et al., 2018).

The envelop of IRF can be obtained using the Hilbert transform. Besides the bridge modal parameters, the bridge displacement at the vehicle-bridge contact-point can be identified from the relevant components by double integration of the bridge related component. Therefore, the flowchart of the proposed drive-by bridge modal identification is shown in Figure 3.

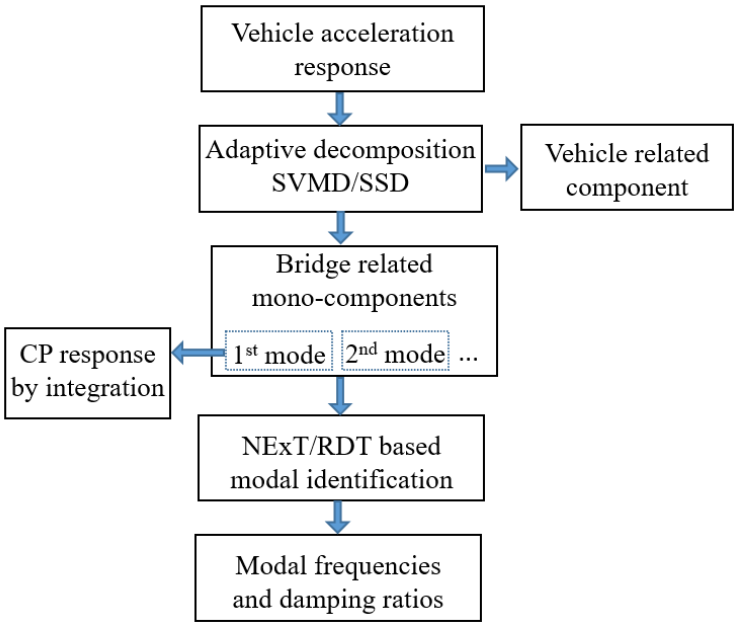

Figure 3 Flow chart of the vehicle response decomposition for drive-by bridge modal identification

4. Numerical study

Numerical study is conducted to analyze the effectiveness of the techniques for extracting mono-components from vehicle responses and drive-by bridge modal identification. The properties of the bridge are: length $L = 35\text{m}$, density $\rho = 5000\,\text{kg/m}$, and flexural rigidity $EI = 2.178\text{e}10\text{Nm}^2$. The damping ratio is set as 0.01 and the theoretical values of the first three bridge modal frequencies are 2.68, 10.71 and 24.09Hz, respectively. The properties of the sensing vehicle are: body mass m_v=466.5kg, suspension stiffness k_s=9.00e5 N/m, suspension damping c_s=0.14e3 N s/m and its fundamental frequency f_v is 6.99Hz. The mass ratio between vehicle and bridge is 0.27% that is small enough to assume that the vehicle does not change the dynamic response of the bridge. The operational load to simulate the traffic on the bridge is a randomly generated white noise load as shown in Figure 4(a) and the sampling frequency is 200Hz. The approach length before the vehicle arriving at the bridge is 35m. When the moving speed of the vehicle is 2m/s, the simulated dynamic responses of the vehicle and the PSD by Fourier transform of the responses considering Class A roughness is presented in Figure 4(b). In the PSD of the response, frequencies f_{b1} and f_{b2} are the first two modal frequencies of the bridge; f_v is the vehicle dynamic frequency.

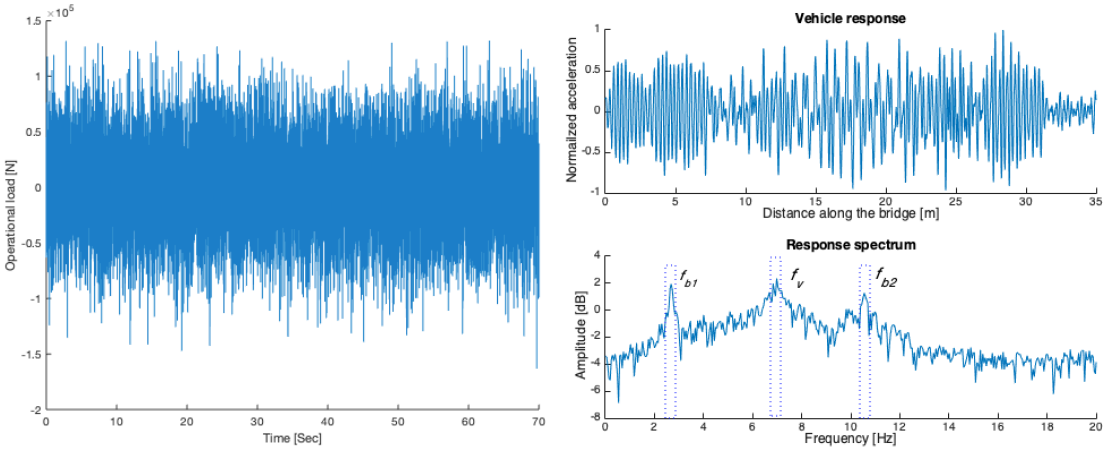

(a) The operational load (b) Vehicle response and PSD of response

Figure 4 The operational load and vehicle response

4.1 Drive-by bridge modal identification using SVMD and SSD

This section is to compare the performance of SVMD and SSD for decomposing the vehicle responses. The noise polluted measurement of the vehicle response is simulated as $y_{noisy}=y_{true}+noise\%\times SD(y_{true})\times WGN$, where y_{true} is the calculated vehicle response; $noise\%$ is the noise level in percentage; $SD(y_{true})$ is the standard deviation of y_{true} and WGN is the standard Gaussian white noise. Noise level of 5% is considered, unless otherwise mentioned. SSD and SVMD are used to decompose the vehicle response respectively. The separated components in time and frequency domains are shown in Figures 5(a) and 5(b), respectively. Four components are obtained from the vehicle response. The first and fourth components are related to the first and second dynamic modes of bridge, respectively. The third component is related to the component of vehicle dynamic response and the second component is related to the driving frequency considering the effect of roughness due to the motion of the sensing vehicle (Yang et al., 2004). It can be seen that the spectrum of driving component is a cluster band with multiple peaks and the amplitude is smaller than that of bridge components.

The results by SSD and SVMD are similar for the extraction of first bridge dynamic mode and vehicle dynamic mode. Moreover, the SVMD can extract the second bridge dynamic component slightly better than SSD as shown in Figure 5(b). The first component is transferred to displacement response by double integration and the result is compared with the contact-point response as shown in Figure 6. It shows that the identified contact responses are very close to the true value.

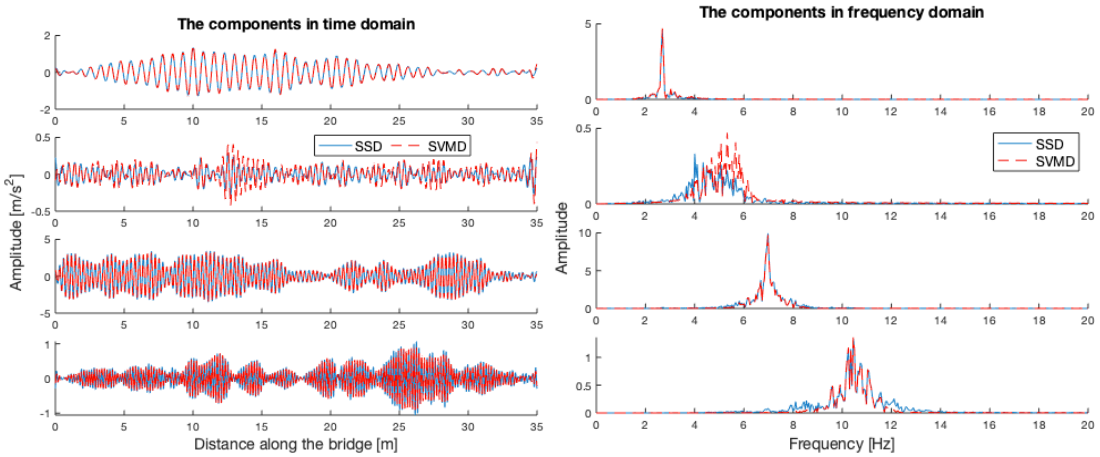

(a) In time domain (b) In frequency domain

Figure 5 The decomposed components by SSD and SVMD

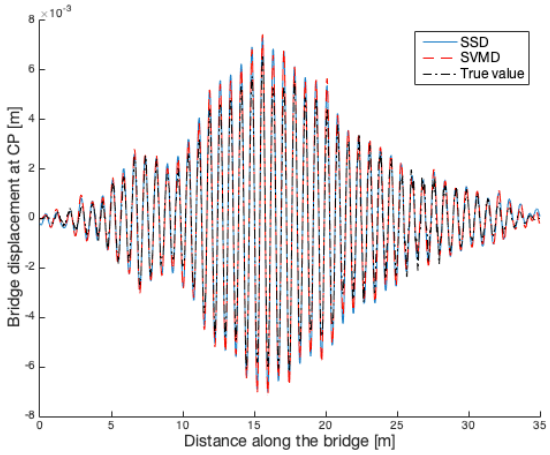

Figure 6 The calculated CP displacement response for Class A road roughness

4.2 Parametric study

4.2.1 Different measurement noise

The effects of the measurement noise on the decomposition performance of the techniques are studied by considering different noise levels to be added into the simulated vehicle acceleration. Three different noise levels are considered, i.e., 0%, 5%, and 15%. The decomposition on the noise polluted measurements is performed using SSD and SVMD respectively. The obtained components and their spectra considering different noise levels are shown in Figures 7 (a) and 7(b), respectively. In the figure, three components related to the first bridge mode, the vehicle mode and the second bridge mode can be clearly identified. The results confirm the robustness of two techniques to the measurement noise. In the rest part of the numerical study, 5% measurement noise is used in the simulation.

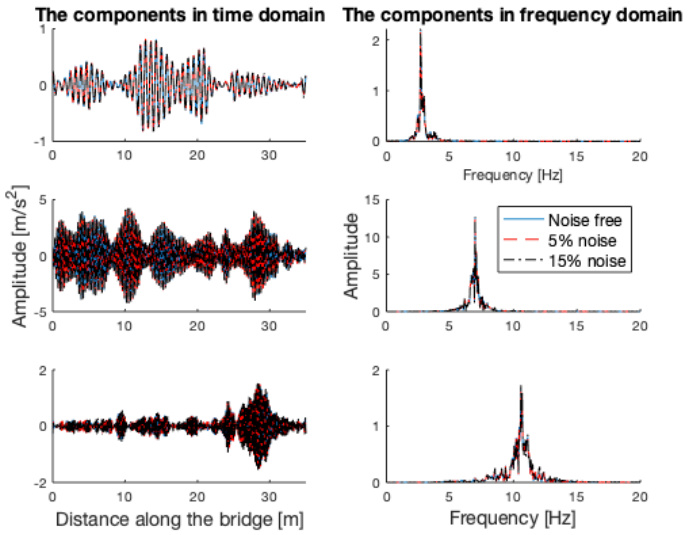

(a) Using SSD

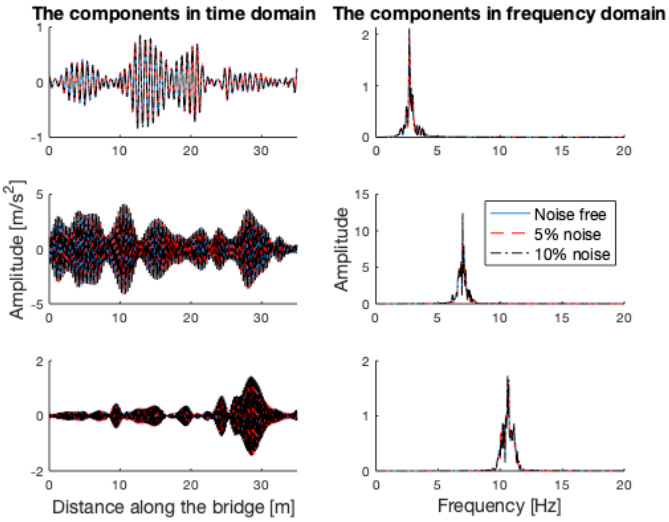

(b) Using SVMD

Figure 7 The decomposed components considering different measurement noise

4.2.2 Effect of the vehicle speed

In the previous study, the vehicle speed is set as 2m/s. To study the effects of vehicle speed on the decomposition, a higher vehicle speed is considered, i.e., 6m/s. SSD and SVMD are used to decompose the vehicle response and the decomposed components are shown in Figure 8 along with their spectra. The results show that only the vehicle related dynamic component is clearly extracted. The components related to the bridge are heavily contaminated due to the effects of surface roughness and higher vehicle speed. Therefore, it is confirmed that a low speed of sensing vehicle is beneficial to the drive-by bridge health monitoring. Moreover, it can be seen that SVMD outperforms SSD in extracting purer modes.

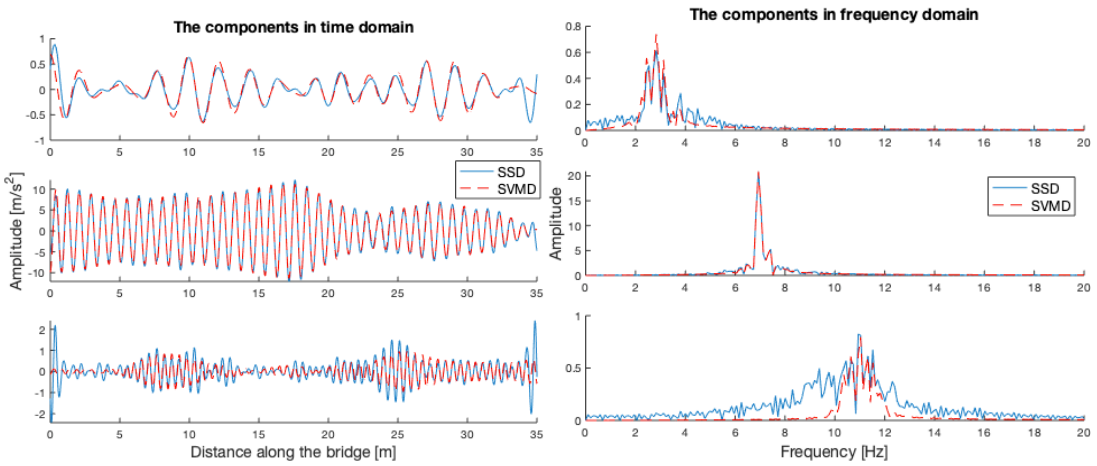

(a) In time domain (b) In frequency domain

Figure 8 The decomposed components in time and frequency domains when vehicle speed is 6m/s

4.2.3 Extraction of close modes between the vehicle and bridge

In above studies the frequency ratio between the vehicle and bridge frequency is 6.99/2.68=2.61. To further study the performance of those two adaptive methods, a close frequency case between the vehicle and bridge is discussed. The stiffness of the vehicle suspension is set as 1/4 of the original value. Therefore, the fundamental frequency of the vehicle becomes 3.49Hz and the frequency ratio between the vehicle and bridge is 1.30. The vehicle response is analyzed using those two methods and the results are shown in Figure 9. Figure 9(a) shows the components and their spectra using SSD and the decomposed components by SVMD are shown in Figure 9(b). In Figure 9(a), the first component is dominated by the first bridge mode, the second component includes both the vehicle and the first bridge modes and there is a clear peak related to the second bridge mode in the third component. The results show that the vehicle and the first bridge modes cannot be separated successfully by SSD. In Figure 19(b), three components are separated successfully and the first, second and third components are related to the first bridge, the vehicle and the second bridge modes respectively. The results show that SVMD can identify both the vehicle and bridge modes for the close mode case.

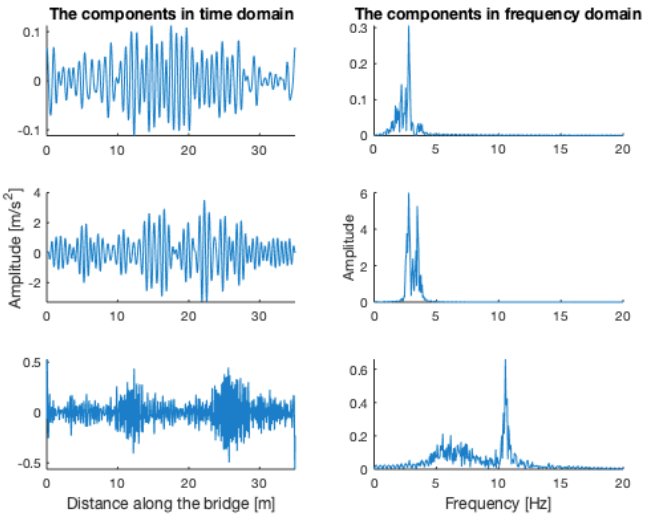

(a) Using SSD

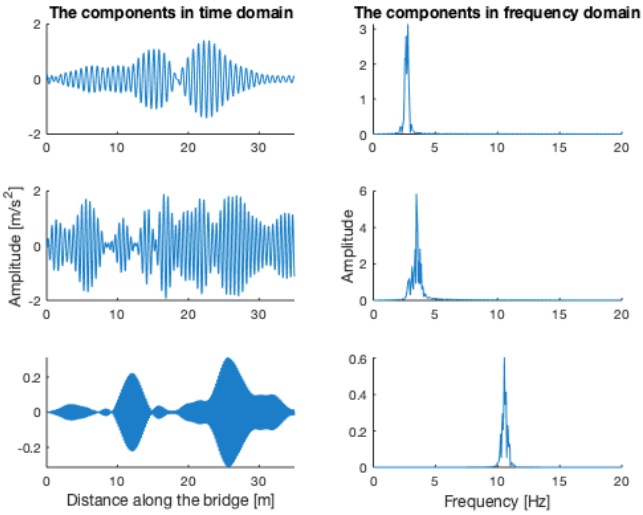

(b) Using SVMD

Figure 9 The decomposed components in time and frequency domains

4.3 Bridge modal parameter identification using multiple passes

The effectiveness of adaptive signal decomposition using SVMD has been discussed in Sections 4.1 and 4.2. This section is to study the bridge modal identification using extracted dynamic components. The dynamic modes decomposed by SVMD are used to extract the bridge frequencies and damping ratios. From the literature, the identification of bridge damping ratios involves more uncertainty and inaccuracy (Yang et al., 2021). To evaluate the accuracy of the proposed drive-by bridge modal identification method, the Monte Carlo method with 50 simulations is used to generate the vehicle response dataset to simulate multiple passes of the sensing vehicle considering random operational load. These responses are analyzed by SVMD, respectively, and the components related to the first two dynamic modes of bridge are used for the identification of frequency and damping ratio. Another two different damping ratio values of bridge, i.e., 0.02 and 0.03 are also considered in the simulating vehicle responses. The mean values and the standard deviation (std) of the identified

frequencies for 50 passes are presented in Table 1. It can be seen that the mean values are very close to the theoretical values and the errors are all less than 1.5%. The results confirm that the bridge modal frequencies can be identified with high accuracy using the developed method.

The curve-fitting modal identification methods based on NExT and RDT are used to estimate the damping ratios from bridge dynamic components. As mentioned in Section 3.2, the time lag T need to be preset. As such, five time lags, $T = ([12, 13, 14, 15, 16]/\ f_{bi}\ )$ are used to identify the damping ratios of the bridge, where f_{bi} is the bridge frequency. Table 2 presents the mean value and standard deviation of the identified damping ratios using the decomposition technique and two damping ratio identification methods with different time lags. It can be seen that the mean value of the damping ratios by multiple passes are close to the true values when damping ratio is 0.01 and 0.02, respectively, and the errors are within 10%. When the damping ratio 0.03 is considered, the maximum error of the damping ratio for the second mode is about 15%. The results show that the proposed method could identify the damping ratio with an acceptable accuracy.

Table 1 Identified frequency considering different damping ratios

Identified frequency (Hz)						
Damping ratio	0.01		0.02		0.03	
	mean	std	mean	std	mean	std
First mode	2.674	0.0561	2.667	0.0419	2.658	0.085
Second mode	10.589	0.0842	10.559	0.1012	10.549	0.182

Table 2 Identified damping ratio considering random operational load

	Damping ratio (%)											True value		Error
T	$12/f_{b1}$		$13/f_{b1}$		$14/f_{b1}$		$15/f_{b1}$		$16/f_{b1}$		Mean	Mode No.	Value (%)	(%)
	mean	std	mean	std	mean	std	mean	std	mean	std				
RDT	1.03	0.48	1.07	0.49	1.09	0.49	1.11	0.49	1.11	0.48	1.08	1st	1.00	8.0
NExT	1.02	0.46	1.04	0.47	1.05	0.48	1.07	0.48	1.08	0.48	1.05	mode		5.0
RDT	0.92	0.51	0.94	0.52	0.95	0.52	0.96	0.52	0.97	0.52	0.95	2nd		5.0
NExT	0.94	0.49	0.96	0.50	0.98	0.51	0.99	0.52	1.00	0.53	0.97	mode		3.0
RDT	2.07	1.00	2.01	0.90	1.94	0.82	1.86	0.76	1.79	0.70	1.93	1st	2.00	2.3
NExT	2.10	0.97	2.00	0.92	1.91	0.87	1.83	0.84	1.77	0.80	1.92	mode		2.7
RDT	1.87	0.67	1.85	0.67	1.82	0.67	1.78	0.67	1.74	0.67	1.81	2nd		9.5
NExT	1.90	0.61	1.91	0.62	1.90	0.62	1.89	0.62	1.86	0.61	1.89	mode		5.5
RDT	3.07	1.79	3.03	1.78	2.98	1.77	2.92	1.73	2.84	1.69	2.97	1st	3.00	1.0
NExT	3.17	1.86	3.15	1.86	3.14	1.87	3.12	1.87	3.10	1.87	3.14	mode		4.7
RDT	2.61	0.86	2.58	0.86	2.54	0.86	2.50	0.85	2.45	0.85	2.54	2nd		15.0
NExT	2.86	0.92	2.82	0.92	2.77	0.92	2.73	0.92	2.68	0.92	2.77	mode		7.7

5. Experimental study on a cable-stayed bridge

In-situ vehicle-bridge interaction test is conducted to further verify the proposed method. The test bridge is a single lane highway bridge with a span 46m and a width 6m (as shown in Figure 10). A long-term monitoring system has been installed on the bridge. The signal condition, data logging software and data logger of the monitoring system were listed in (Sun et al., 2017). The dynamic monitoring system continuously records the vibration response of the bridge and produces a file with an acceleration time series every 10 minutes at a sample rate of 600Hz. A dense array of accelerometers is installed under the bridge deck and timely synchronized to measure the structure responses. Figure 10(b) shows the locations of the installed 24 accelerometers on the deck. The measured data are continuously transferred over a 4G cellular network to the database.

(a) The cable-stayed bridge

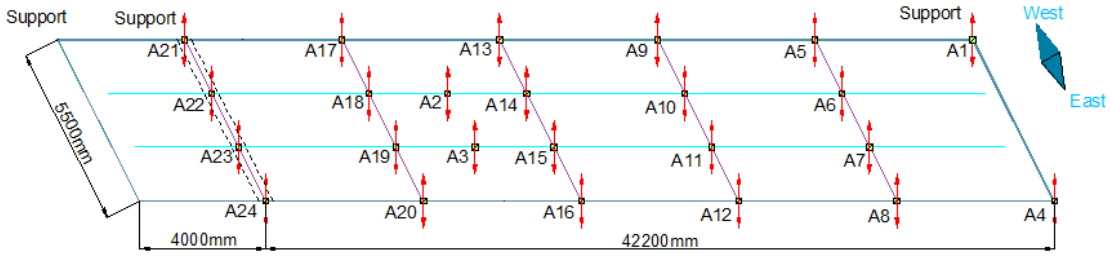

(b) Sensor location on the bridge deck

Figure 10 Long-term monitoring of a cable-stayed bridge

5.1 Bridge modal identification

Bridge modal analysis is conducted using the responses measured from the accelerometers on the bridge deck. Bridge acceleration responses measured after a vehicle excitation are analyzed with modal analysis toolbox from Chang et al. (2012) for the identification of bridge modal parameters. Figure 11 gives the identified bridge vibration modes including the modal frequencies. For the vibration after the vehicle excitation, six vibration modes are identified. It can be seen that the first bridge vibration mode at 2.03Hz is the vertical bending mode of the deck and the mode at 5.86Hz is the third vertical bending mode. The other modes show a mixture of torsion and bending.

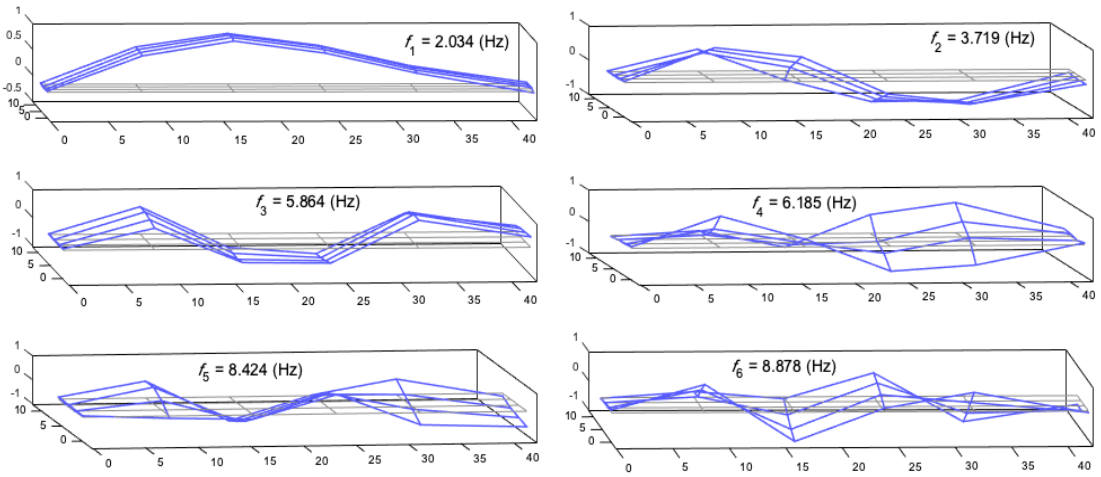

Figure 11 Identified bridge vibration modes

5.2 Bridge modal identification

For the bridge modal identification test, a vehicle of Hyundai Tucson 2006 model with a gross weight of 1.5t is used. A wireless accelerometer (manufactured by BeanAir) is installed on the top surface of the dashboard as shown in Figure12. The vehicle responses are measured when it stops on the ground and on the bridge deck with its engine idling, respectively. Figure 13 shows the measured responses and their spectra. The results show that there are two dominated peaks at 17.5Hz and 23.3Hz in the spectrum and they are the vehicle engine-related frequencies as it is idling. In the results when the vehicle parks on the bridge deck, the peak at 2.0Hz is also visible and that is related to the first bridge vibration mode. The vehicle is driven multiple times on the ground with different speeds at 10, 20 and 30km/h, respectively. The dynamic responses measured from the wireless sensor are used for spectrum analysis with Fourier transform. After analyzing all the responses, the first three vibration frequencies of the vehicle body when it is moving are 1.2, 1.5~1.8 and 2.2~2.7 Hz, respectively.

The dynamic response measured from the wireless sensor when the vehicle passes the bridge at a speed 10km/h is shown in Figure 14. SVMD and SSD are used to decompose the vehicle response and Figures 15(a) and 15(b) show the decomposed components and their spectra, respectively. In Figure 15(a), five components are extracted using SVMD. The first two components are around 1.05Hz and 1.56Hz and they are related to the vehicle dynamic responses. Other three components are around 2.05Hz, 3.56Hz and 6.23Hz. Compared with the results using sensors on the bridge, these three components are corresponding to the first, second and fourth dynamic modes of the bridge respectively. The results show that the SVMD can successfully extract the bridge related dynamic components from vehicle response. Figure 15(b) shows three components extracted by SSD. The results show that the bridge related components are not extracted successfully. This further confirms the numerical results that the SVMD can decompose the mono-components from the vehicle responses when the frequencies of the vehicle and bridge are close.

(a) Vehicle used for the test (b) Vehicle instrumentation

Figure 12 Vehicle for test and instrumentation with wireless sensor

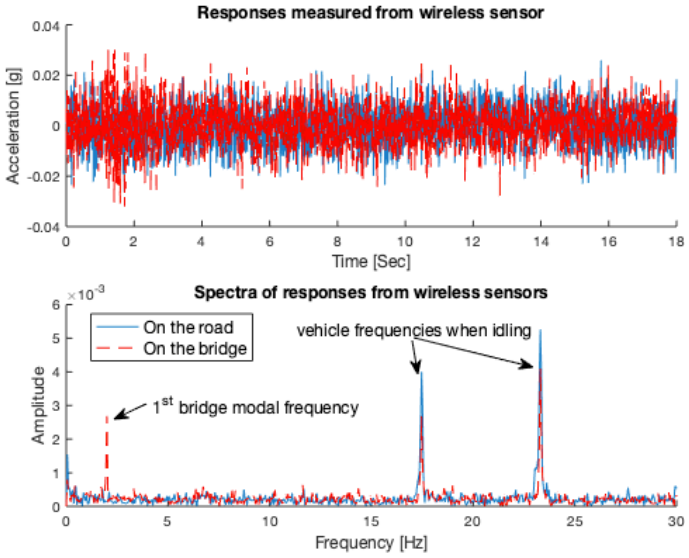

Figure 13 Response measurements when vehicle stops on the road and bridge

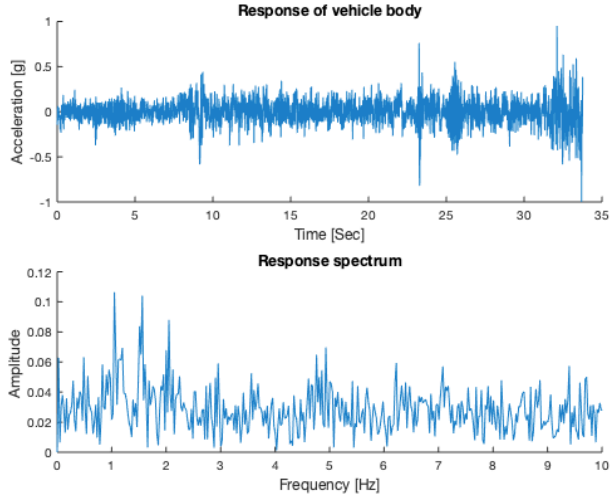

Figure 14 Response measured in the vehicle and the response spectrum

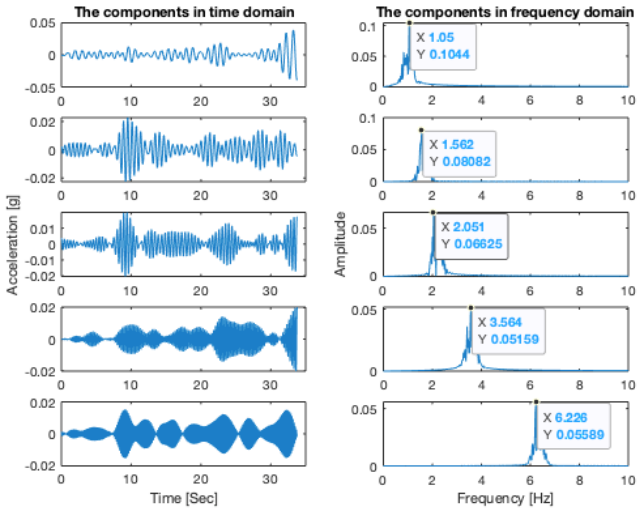

(a) Using SVMD

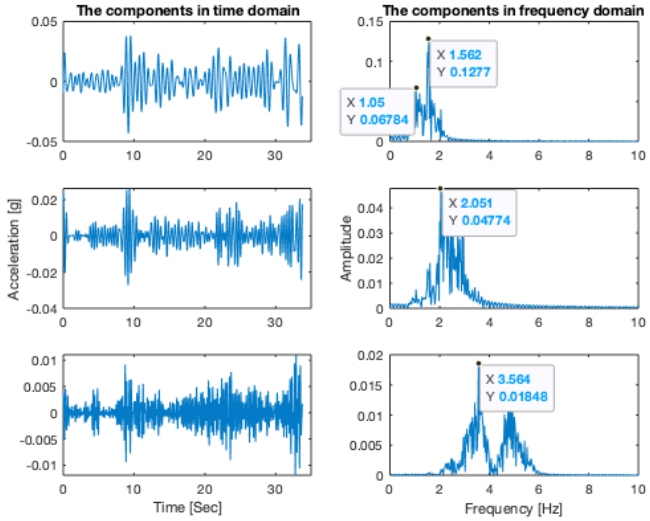

(b) Using SSD

Figure 15 The decomposed components using SVMD and SSD

6 Conclusions

This study investigates the adaptive decomposition of responses of moving vehicle for bridge modal identification using SVMD. The performance of SVMD is compared to that of SSD. Results of the parametric analysis demonstrate that the techniques can extract the mono-components from vehicle responses. It is also found that the components extracted from vehicle response by using the adaptive decomposition techniques can be further analyzed to get contact-point displacement response of the bridge. Numerical and experimental study confirms that the SVMD performs better than the SSD, especially when the frequencies of the components in the vehicle response are close.

For the bridge modal identification from a moving test vehicle, the NExT and RDT based modal identifications are both incorporated to analyze the bridge related dynamic components to estimate the modal frequencies and damping ratios. The bridge modal parameters are identified accurately by computing the mean value of multiple tests

when the damping ratio is 0.01 and 0.02, respectively. The damping ratio identification is more sensitive to the operational load than the frequency identification and the multiple tests can improve the accuracy of damping ratio identification when the bridge is subjected to random operational load.

Acknowledgements

This research is supported in part by research funding of the National Natural Science Foundation of China (U1709207, 52078461, 52108288, 51878433), Key R&D program of Zhejiang (2019C03098) and Zhejiang Provincial Postdoctoral Science Foundation (ZJ2020024). The financial aid is gratefully acknowledged.

[1] **Reference**

Bonizzi, P., Karel, J. M. H., Meste, O., and Peeters, R. L. M. (2014). Singular spectrum decomposition: a new method for time series decomposition. *Advances in Adaptive Data Analysis*, 06(04), 1450011.

Chang, M., Pakzad, S. N., and Leonard, R. (2012). Modal identification using SMIT. *Topics on the Dynamics of Civil Structures.* Springer, 221-228.

Dragomiretskiy, K., and Zosso, D. (2014). Variational mode decomposition. *IEEE Transactions on Signal Processing*, 62(3), 531-544.

Elsner, J. B. and Tsonis, A. A. (1996). Singular spectrum analysis, a new tool in time series analysis. Springer, New York.

Fu, J. J., Cai, F. Y., Guo, Y. H., Liu, H. D., and Niu, W. T. (2020). An improved VMD-based denoising method for time domain load signal combining wavelet with singular spectrum analysis. *Mathematical Problems in Engineering*, 2020, 1485937.

Henchi, K., Fafard, M., Talbot, M., and Dhatt, G. (1998). An efficient algorithm for dynamic analysis of bridges under moving vehicles using a coupled modal and physical components approach. *Journal of Sound and Vibration*, 212(4), 663-683.

Hester, D., and González, A. (2017). A discussion on the merits and limitations of using drive-by monitoring to detect localised damage in a bridge. *Mechanical Systems and Signal Processing*, 90, 234-253.

Ibrahim, S. R. (1977). Random decrement technique for modal identification of structures. *Journal of Space craft and Rockets*, 14(11), 696-700.

ISO-8608 (1995), *Mechanical Vibration-Road Surface Profiles-Reporting of Measured Data*, International Organization for Standardization (ISO), Geneva.

James, G. H., Carne, T. G., and Lauffer, J. P. (1993). The natural excitation technique (NExT) for modal parameter extraction from operating wind turbines. *Technical Report: SAND92-1666, UC-261*, Sandia National Laboratories, Albuquerque, New Mexico.

Jian, X. D., Xia, Y., and Sun, L. M. (2020). An indirect method for bridge mode shapes identification based on wavelet analysis. *Structural Control and Health Monitoring*, 27(12), e2630.

Kildashti, K., Makki Alamdari, M., Kim, C. W., Gao, W., and Samali, B. (2020). Drive-by-bridge inspection for damage identification in a cable-stayed bridge: Numerical investigations. *Engineering Structures*, 223, 110891.

Kong, X., Cai, C. S., and Kong, B. (2014). Damage detection based on transmissibility of a vehicle and bridge coupled system. *Journal of Engineering Mechanics*, 141(1), 04014102.

Kordestani, H., Xiang, Y. Q., Ye, X. W., Jia, Y. K. (2018). Application of the random decrement technique in damage detection under moving load. *Applied Sciences*, 8(5), 753.

Li, F., Zhang, B., Verma, S., and Marfurt, K. J. (2018). Seismic signal denoising using thresholded variational mode decomposition. *Exploration Geophysics,* 49(4), 450-461.

Li, J. T., Guo, J., and Zhu, X. Q. (2021). Time-varying parameter identification of bridges subject to moving vehicles using ridge extraction based on empirical wavelet transform. *International Journal of Structural Stability and Dynamics*, 21(04), 2150046.

Li, J. T., Zhu, X. Q., Law, S.S., and Samali, B. (2019). Drive-by blind modal identification with singular spectrum analysis. *Journal of Aerospace Engineering*, 32(4), 04019050.

Li, Y., Chen, X., Yu, J., and Yang, X. (2019). A fusion frequency feature extraction method for underwater acoustic signal based on variational mode decomposition, duffing chaotic oscillator and a kind of permutation entropy. *Electronics,* 8(1), 61.

Locke, W., Sybrandt, J., Redmond, L., Safro, I., and Atamturktur, S. (2020). Using drive-by health monitoring to detect bridge damage considering environmental and operational effects. *Journal of Sound and Vibration*, 468, 115088.

Makki Alamdari, M., Chang, K. C., Kim, C. W., Kildashti, K., and Kalhori, H. (2021). Transmissibility performance assessment for drive-by bridge inspection. *Engineering Structures*, 242, 112485.

Mei, Q. P., Gül, M., and Boay, M. (2019). Indirect health monitoring of bridges using Mel-frequency cepstral coefficients and principal component analysis, *Mechanical System and Signal Processing*, 119, 523-546.

Nazari, M., and Sakhaei, S. M. (2018). Variational mode extraction: a new efficient method to derive respiratory signals from ECG. *IEEE Journal of Biomedical and Health Informatics*, 22(4), 1059-1067.

Nazari, M., and Sakhaei, S. M. (2020). Successive variational mode decomposition. *Signal Processing*, 174, 107610.

Ni, P. H., Li, J., Hao, H., Xia, Y., Wang, X. Y., Lee, J. M., and Jung, K. H. (2018). Time-varying system identification using variational mode decomposition. *Structural Control and Health Monitoring,* 25(6), e2175.

O'Brien, E. J., Malekjafarian, A., and González, A. (2017). Application of empirical mode decomposition to drive-by bridge damage detection. *European Journal of Mechanics - A/Solids*, 61, 151-163.

Sadeghi Eshkevari, S., Matarazzo, T. J., and Pakzad, S. N. (2020). Simplified vehicle–bridge interaction for medium to long-span bridges subject to random traffic load. *Journal of Civil Structural Health Monitoring*, 10(4), 693-707.

Sun M, Makki Alamdari M and Kalhori H. (2017). Automated operational modal analysis of a cable-stayed bridge. *Journal of Bridge Engineering*, 22(12): 05017012.

Tan, C. J., Elhattab, A., and Uddin, N. (2020). Wavelet-entropy approach for detection of bridge damages using direct and indirect bridge records. *Journal of Infrastructure Systems,* 26(4), 04020037.

Tan, C. J., Uddin, N., O'Brien, E. J., McGetrick, P. J., and Kim, C. W. (2019). Extraction of bridge modal parameters using passing vehicle response. *Journal of Bridge Engineering*, 24(9), 04019087.

Tian, Y. D., and Zhang, J. (2020). Structural flexibility identification via moving-vehicle-induced time-varying modal parameters. *Journal of Sound and Vibration*, 474, 115264.

Wu, Z., and Huang, N. E. (2009). Ensemble empirical mode decomposition: a noise-assisted data analysis method. *Advances in Adaptive Data Analysis*, 01(01), 1-41.

Yang, J. P., and Lee, W. C. (2018). Damping effect of a passing vehicle for indirectly measuring bridge frequencies by EMD technique. *International Journal of Structural Stability and Dynamics*, 18(01), 1850008.

Yang, Y. B., and Chang, K. C. (2009). Extraction of bridge frequencies from the dynamic response of a passing vehicle enhanced by the EMD technique. *Journal of Sound and Vibration, 322*(4–5), 718-739.

Yang, Y. B., Chang, K. C., and Li, Y. C. (2013). Filtering techniques for extracting bridge frequencies from a test vehicle moving over the bridge. *Engineering Structures*, 48, 353-362.

Yang, Y. B., Lin, C. W., and Yau, J. D. (2004). Extracting bridge frequencies from the dynamic response of a passing vehicle. *Journal of Sound and Vibration*, 272(3): 471-493.

Yang, Y. B., Shi, K., Wang, Z. L., Xu, H., Zhang, B., and Wu, Y. T. (2021). Using a Single-DOF test vehicle to simultaneously retrieve the first few frequencies and damping ratios of the bridge. *International Journal of Structural Stability and Dynamics*, 2150108.

Yang, Y. B., Wang, Z. L., Shi, K., Xu, H., and Wu, Y. T. (2020). State-of-the-art of vehicle-based methods for detecting various properties of highway bridges and railway tracks. *International Journal of Structural Stability and Dynamics*, 20(13), 2041004.

Zhang, X., Miao, Q., Zhang, H., and Wang, L. (2018). A parameter-adaptive VMD method based on grasshopper optimization algorithm to analyze vibration signals from rotating machinery. *Mechanical Systems and Signal Processing*, 108, 58-72.

Zhu, L., and Malekjafarian, A. (2019). On the use of ensemble empirical mode decomposition for the identification of bridge frequency from the responses measured in a passing vehicle. *Infrastructures,* 4(2), 32.